



HAL
open science

Tracking ionic fluxes in porous carbon electrodes from aqueous electrolyte mixture at various pH

Yih-Chyng Wu, Pierre-Louis Taberna, Patrice Simon

► **To cite this version:**

Yih-Chyng Wu, Pierre-Louis Taberna, Patrice Simon. Tracking ionic fluxes in porous carbon electrodes from aqueous electrolyte mixture at various pH. *Electrochemistry Communications*, 2018, 93, pp.119-122. 10.1016/j.elecom.2018.06.014 . hal-02025005

HAL Id: hal-02025005

<https://hal.science/hal-02025005>

Submitted on 19 Feb 2019

HAL is a multi-disciplinary open access archive for the deposit and dissemination of scientific research documents, whether they are published or not. The documents may come from teaching and research institutions in France or abroad, or from public or private research centers.

L'archive ouverte pluridisciplinaire **HAL**, est destinée au dépôt et à la diffusion de documents scientifiques de niveau recherche, publiés ou non, émanant des établissements d'enseignement et de recherche français ou étrangers, des laboratoires publics ou privés.



Open Archive Toulouse Archive Ouverte (OATAO)

OATAO is an open access repository that collects the work of Toulouse researchers and makes it freely available over the web where possible

This is an author's version published in: <http://oatao.univ-toulouse.fr/21776>

Official URL: <https://doi.org/10.1016/j.elecom.2018.06.014>

To cite this version:

Wu, Yih-Chyng[✉] and Taberna, Pierre-Louis[✉] and Simon, Patrice[✉]
Tracking ionic fluxes in porous carbon electrodes from aqueous electrolyte mixture at various pH. (2018) *Electrochemistry Communications*, 93. 119-122. ISSN 1388-2481

Any correspondence concerning this service should be sent to the repository administrator: tech-oatao@listes-diff.inp-toulouse.fr

Tracking ionic fluxes in porous carbon electrodes from aqueous electrolyte mixture at various pH

Yih-Chyng Wu, Pierre-Louis Taberna, Patrice Simon*

Université Paul Sabatier, CIRIMAT UMR CNRS 5085, 118 route de Narbonne, 31062 Toulouse, France
Réseau sur le Stockage Electrochimique de l'Energie (RS2E), FR CNRS 3459, France

ARTICLE INFO

Keywords:

Electrochemical quartz crystal microbalance
Supercapacitor
Microporous carbon
Ion dynamics
Energy storage

ABSTRACT

Electrochemical quartz crystal microbalance (EQCM) and cyclic voltammetry (CV) techniques were used to study ion dynamics in porous carbide-derived carbon (CDC) electrodes in various aqueous electrolytes. Although the cyclic voltammograms look similar, EQCM revealed different ion transfer depending on the electrolyte during both positive and negative polarization. During polarization in neutral K_2SO_4 electrolyte, partial desolvation of cation and anion were observed in carbon micropores. In $\text{EMI}^+\text{-HSO}_4^-$ electrolyte, the main charge carrier during cation adsorption was not found to be bulkier EMI^+ , but smaller and highly mobile H^+ . Furthermore, ionic fluxes during charging/discharging were monitored and identified in multi-ions aqueous system, which was ambiguous according to the CV plots. EQCM shows its powerful ability to serve as an accurate gravimetry probe to study the electrolyte concentration and compositional changes in porous materials.

1. Introduction

The development of modern societies highly relies on energy [1]. One of the promising energy storage devices is electrochemical double layer capacitors (EDLCs), also known as supercapacitors [2–4]. In EDLCs, high capacitance can be reached by using high specific surface area active porous carbon materials for charging the electrochemical double layer capacitance [5–9].

Carbide derived carbons (CDCs) have been one of the most attractive model materials for EDLC applications because of tunable pore size and narrow pore size distribution [10–14]. Significant research works have revealed that the capacitance increased dramatically when the carbon pore size was decreased below the solvated ion size [15–17]. Later on, other works have been done to understand ion transport and solvation effect from various electrolytes confined in nanoporous materials aiming for improving the performance of supercapacitor electrode [18–23].

Electrochemical quartz crystal microbalance (EQCM) has been used as an in-situ gravimetric probe for investigating the ion dynamics in porous materials [17,19,20,24–28]. However, none of the previous works had extended the discussion to complex mixture of ions in aqueous electrolyte.

In this work, ion dynamics in multi-ion aqueous electrolytes have been investigated by EQCM in gravimetric mode using titanium carbide derived carbon (TiC-CDC) as active material in 0.1 M K_2SO_4 aqueous

solution, 0.1 M $\text{EMI}^+\text{-HSO}_4^-$ aqueous solution and a mixture containing 0.1 M of K_2SO_4 and $\text{EMI}^+\text{-HSO}_4^-$. The study of main charge carriers in multi-ion aqueous electrolytes during ion transfer and adsorption in carbon micropores have been achieved and explained in this study based on ion size, ion mobility and pH range.

2. Experimental

TiC-CDC porous carbon sample has a BET surface area of $1820 \text{ m}^2\text{g}^{-1}$ and mean pore diameter of 0.7 nm [29]. Maxtek 1-in.-diameter Au-coated quartz crystals (oscillating frequency, f_0 , 5 MHz) were coated by drip-coating using a precise pipette with a slurry containing 80 wt% of TiC-CDC mixed with 20 wt% of polyvinylidene fluoride binder in N-Methyl-2-pyrrolidone [30]. The loading of TiC-CDC was controlled around 40 to 60 $\text{ng}\cdot\text{cm}^{-2}$. The coated quartz crystal was dried in an oven at 60 °C for overnight. The coated quartz crystal was used as the working electrode in a 3-electrode cell, together with a $\text{Hg}/\text{Hg}_2\text{SO}_4$ reference electrode and a Pt counter electrode. EQCM electrochemical measurements were carried out using a Maxtek RQCM system combined with Autolab PGSTAT101. The potential of zero charge (pzc) was found by measuring the minimum capacitance from cyclic voltammogram with three-electrode Swagelok cell [30], using a TiC-CDC working electrode of 0.8 to 1.7 $\text{mg}\cdot\text{cm}^{-2}$ and an over capacitive counter electrode of porous carbon film (23 $\text{mg}\cdot\text{cm}^{-2}$). For the EQCM results, the electrode mass change was calculated using

* Corresponding author at: CIRIMAT, Université de Toulouse, CNRS, INPT, UPS, 118, Route de Narbonne, 31062 Toulouse cedex 9, France.
E-mail address: simon@chimie.ups-tlse.fr (P. Simon).

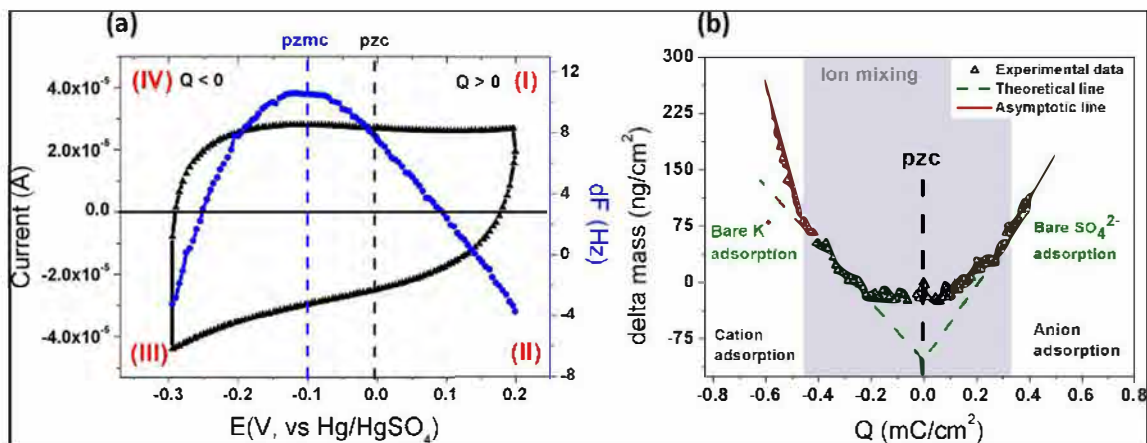


Fig. 1. (a) CV and EQCM frequency response of CDC-0.7 nm carbon electrode in 0.1 M K_2SO_4 aqueous electrolyte at $10\text{ mV}\cdot\text{s}^{-1}$. (b) Electrode mass change vs charge during the polarization of CDC-0.7 nm in 0.1 M K_2SO_4 aqueous electrolyte. Black solid marks are measured mass change (EQCM), green dashed lines are the theoretical mass change of neat ions. The red solid line shows the linear fitting of measured mass change. (For interpretation of the references to color in this figure legend, the reader is referred to the web version of this article.)

Sauerbrey equation: $\Delta m = -C_f \Delta f$, where Δm is the change of mass of the coating and C_f is the sensitivity factor of the crystal. C_f was calculated to $14.6\text{ ng}\cdot\text{Hz}^{-1}$ (or $11.496\text{ ng}\cdot\text{Hz}^{-1}\text{ cm}^{-2}$ taking into account the Au crystal electrode surface of 1.27 cm^2). Blank tests achieved using uncoated quartz led to a current density below $0.01\text{ }\mu\text{A}/\text{cm}^2$ within the potential range studied. Three CVs cycles were run before starting EQCM measurements, to start from stable, reproducible electrochemical signature.

3. Results and discussion

Fig. 1a (black line) shows the cyclic voltammogram (CV) of a TiC-CDC carbon electrode in 0.1 M K_2SO_4 aqueous electrolyte recorded from EQCM set-up at a scan rate of $10\text{ mV}\cdot\text{s}^{-1}$, from -0.3 to 0.2 V vs Ref. The associated frequency response (Δf vs E) measured by EQCM is shown in blue solid marks. The rectangular CV profile is characteristic of a capacitive behavior. The potential of zero charge (pzc) and potential of zero mass change (pzmc) are indicated in black and blue dashed line, respectively. The pzc refers to a potential at which surface net charge of the electrode is null and was, accordingly, taken as the zero charge in the plots ($\Delta Q = 0\text{ mC}/\text{cm}^2$ at pzc). The pzmc is the potential at the minimum mass change in Δm vs E plot that the maximum of the Δf vs E plot (see Sauerbrey equation). A difference of pzc and pzmc values indicates a failure of permselectivity behavior in carbon [25]. This is associated with a difference in ion mobility of cations and anions of the electrolyte confined in pores, leading to a cation-anion mixing zone near pzc. Although the electrode weight change is fully reversible within one CV cycle, there is hysteresis in the frequency response of the electrode when crossing the pzc [25], due to the ion mixing zone. Since this ion mixing zone is kinetically controlled and enlarged when the electrode potential crosses the pzc [25], the results in Fig. 1b were obtained from separate scans from pzc to cathodic potentials and from pzc to anodic potentials to study cation and anion adsorption, respectively. Fig. 1b shows the experimental change of the electrode weight (Δm) vs the charge (ΔQ) passed in the electrode during ion charging in cyclic voltammetry. Theoretical curves (dashed green lines in Fig. 1b) are calculated from Faraday's law, assuming one electrode charge is counterbalanced by one counter-ion. As a result, the slope in the negative charge region is the molar weight of bare K^+ ion ($M = 39\text{ g}\cdot\text{mol}^{-1}$) and the one of SO_4^{2-} ion ($M = 96\text{ g}\cdot\text{mol}^{-1}$) for positive charge. The grey area indicates ion mixing zone, that is where the slope of experimental mass changes versus charge is less than the theoretical one (dashed green lines). The red lines reported in Fig. 1b represent the region where ion exchange is minimum, that is at high

positive or negative charge Q . The calculated experimental average molecular weights of the adsorbed species are $134\text{ g}\cdot\text{mol}^{-1}$ for negative polarization (cation region) and $115\text{ g}\cdot\text{mol}^{-1}$ for positive polarization (anion region), respectively. Assuming that the difference between average molecular weights and bare ion molecular weight is attributed solely to water molecules surrounding the ion, the hydration number of each ion could be estimated as 5.3 for K^+ and 0.9 for SO_4^{2-} . For sake of comparison, the bulk solution hydration number of K^+ and SO_4^{2-} were reported to be 7 and 13, respectively [31–33]. Thus, for both cations and anions, partial ion desolvation was observed, but in less extent regarding K^+ ions since the calculated hydration number is close to the bulk solution hydration number. This might be due to the small size of the hydrated potassium ion which its diameter is reported as 0.66 nm [34]. It is very close to the pore size of TiC-CDC (0.7 nm) used here as active material. For larger SO_4^{2-} ions, the value of calculated hydration number is very close to 1 indicating desolvation for anions in the carbon micropores, in agreement with the large size of hydrated SO_4^{2-} ion (0.76 nm) [35].

In a next step, K^+ cations were replaced with larger EMI^+ cations by using i) a solution of 0.1 M $EMI\text{-HSO}_4$ ($\text{pH} = 0.8$) and ii) a mixture of 0.1 M K_2SO_4 and 0.1 M $EMI^+\text{-HSO}_4^-$ ($\text{pH} = 1.2$). Note that the pH of the solution has been changed to bring new insights regarding the charge process mechanism when various cations are likely to be involved.

CVs recorded using three-electrode Swagelok cells were found very similar in both electrolytes (Fig. 2a). Fig. 2b shows the Δm versus ΔQ plot recorded by EQCM during the polarization of TiC-CDC electrode sample in 0.1 M $EMI^+\text{-HSO}_4^-$. The calculated experimental molecular weights in the high positive and negative charge Q regions (as shown in red lines in Fig. 2b) for anion and cation were found to be $31\text{ g}\cdot\text{mol}^{-1}$ and $1.3\text{ g}\cdot\text{mol}^{-1}$ per charge, respectively. Compared to neutral K_2SO_4 aqueous electrolyte, the composition of cations in $\text{pH} = 0.8$ $EMI^+\text{-HSO}_4^-$ electrolyte is more complex. In such acidic electrolyte, protons and hydrated protons (H_3O^+) ions are present. According to Fig. 2b, no weight change was observed at high negative charge density. Considering the molecular weight of EMI^+ cation ($111\text{ g}\cdot\text{mol}^{-1}$), the possibility of EMI^+ adsorption seems unlikely. Previous literature reported that EMI^+ cations could access confined pores of 1 nm by partial desolvation in acetonitrile based electrolyte [20]. However, in the present $\text{pH} = 0.8$ aqueous electrolyte, EMI^+ cation mobility is much slower than protons, so that they are not involved in the charge process. This strongly suggests protons ($M = 1\text{ g}\cdot\text{mol}^{-1}$) to be the main charge carriers during cation adsorption via Grotthuss mechanism [36]. At moderate negative charge, an ion mixing zone is observed.

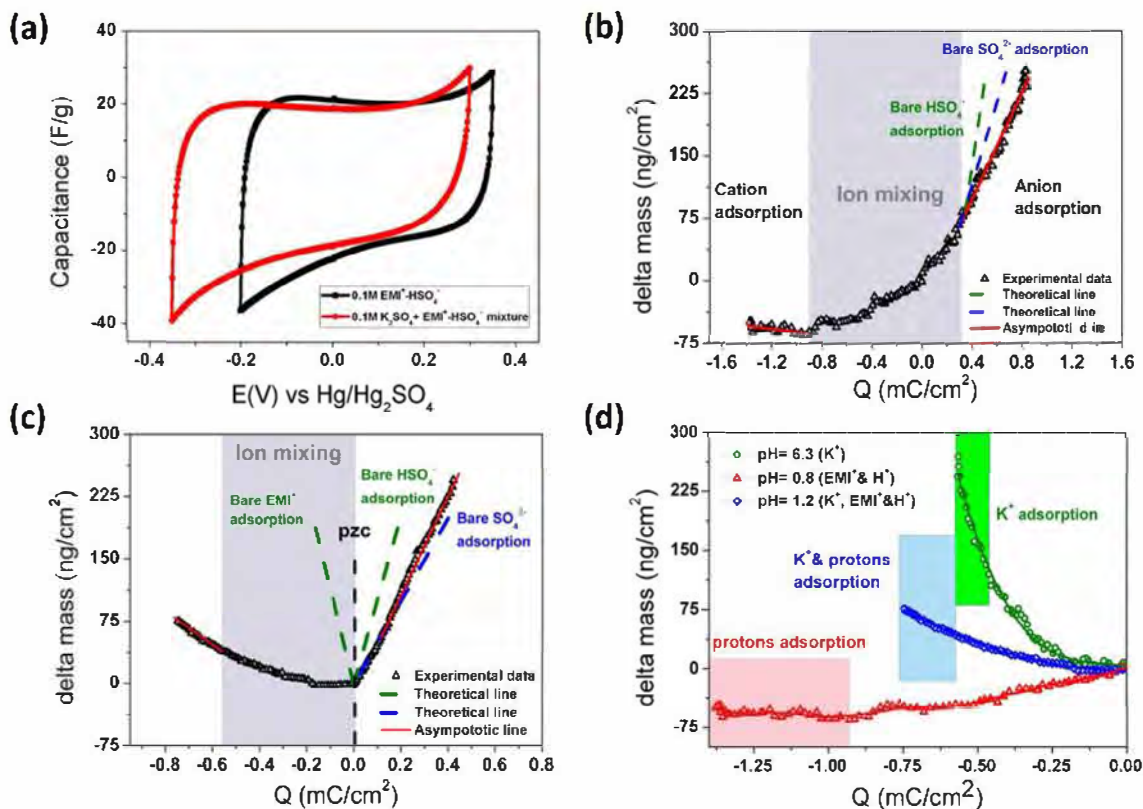


Fig. 2. (a) CVs of CDC-0.7 nm carbon electrode in 0.1 M EMI^+ - HSO_4^- aqueous electrolyte and a mixture of 0.1 M K_2SO_4 and 0.1 M EMI^+ - HSO_4^- tested in three-electrode Swagelok cell at 5 mV s^{-1} . (b) Electrode mass change vs charge during the polarization of CDC-0.7 nm in 0.1 M EMI^+ - HSO_4^- aqueous electrolyte (pH = 0.8). (c) Electrode mass change vs charge during the polarization of CDC-0.7 nm in mixture of 0.1 M K_2SO_4 and 0.1 M EMI^+ - HSO_4^- aqueous electrolyte (pH = 1.2). (d) Comparison of electrode mass change versus charge density for different electrolytes with TiC-CDC electrode material from $Q = 0 \text{ mC/cm}^2$ to negative charge density. (For interpretation of the references to color in this figure, the reader is referred to the web version of this article.)

For positive charge ($Q > 0$), Fig. 2b shows an increase of mass change in carbon micropores. The calculated molecular weight per charge ($31 \text{ g}\cdot\text{mol}^{-1}$) is less than that of bare HSO_4^- anion ($97 \text{ g}\cdot\text{mol}^{-1}$). It is also smaller than that of SO_4^{2-} anion ($48 \text{ g}\cdot\text{mol}^{-1}$), even though SO_4^{2-} anion adsorption should not be pre-dominant because of the low pH value of the electrolyte. This means that not only adsorption of solvated anion occurs in micropores, but also cation desorption [37], which is hydrated proton in this experiment.

The results of the gravimetric study in a mixture of 0.1 M K_2SO_4 and 0.1 M EMI^+ - HSO_4^- electrolytes at pH = 1.2 are shown in Fig. 2c. The frequency change in the negative charge range (Fig. 2c) is smaller than that of the positive charge density domain. In mixed electrolyte, the composition of cations (K^+ , EMI^+ , H^+ , H_3O^+) and anions (HSO_4^- and SO_4^{2-}) are more complex than previous cases. Since the valence state of anions are different, the calculated molecular weights were normalized to the charge for better comparison. The calculated experimental average molecular weight per charge for cation and anion is 17 and $58 \text{ g}\cdot\text{mol}^{-1}$, respectively (red lines in Fig. 2c). For $Q > 0$ since no ion-mixing phenomena was observed, only anion adsorption is considered. According to previous results obtained in K_2SO_4 electrolyte, the calculated hydration number for sulfate anion is between 0 and 1, which indicates almost bare sulfate ions adsorbed into carbon micropores. Due to a higher valence state of sulfate anion than HSO_4^- bisulfate ion, more energy will be needed for desolvation of water molecules while entering carbon micropores. As a result, bare bisulfate anion access to TiC-CDC micropores can be expected. This supports the existence of a mix of sulfate and bisulfate anions adsorbed into TiC-CDC carbon micropores from pzc to positive charge density. From direct calculation, the contribution of sulfate anion and bisulfate anion can be estimated to 80% and 20%, respectively, during the anion adsorption

process. For high negative charge ($Q < 0$), the calculated average molecular weight per charge ($17 \text{ g}\cdot\text{mol}^{-1}$) is much smaller than K^+ and EMI^+ cations. Fig. 2d summarizes all the results obtained in the different electrolytes with TiC-CDC electrode material scanned at the same scan rate in the negative charge range.

As shown in Fig. 2d, in the negative charge density range, both electrolytes containing K^+ cations show an increase of mass change (green and blue line in Fig. 2d). However, the weight change of mixed electrolyte (blue) is smaller than in neutral K_2SO_4 electrolyte, that is without the presence of bulky EMI^+ cation. The slow increase of electrode mass at low negative charge density ($Q = 0$ to $-0.6 \text{ mC}\cdot\text{cm}^{-2}$) in the mixed electrolyte is caused by ion-mixing. Then, at high negative charge density ($Q < -0.6 \text{ mC}\cdot\text{cm}^{-2}$), it is confirmed that K^+ ($39 \text{ g}\cdot\text{mol}^{-1}$) is not the only cation involved in the charge process, based on the calculated experimental molecular weight ($17 \text{ g}\cdot\text{mol}^{-1}$). In the electrolyte mixture at pH = 1.2, the potassium molar ionic conductivity is in the range of proton's one (which is not the case for EMI^+). This explains that the calculated average molecular mass per charge is found between the theoretical molecular weight of proton and potassium at pH equals to 1.2. From direct calculation, the contribution of proton and potassium cation is 44% and 56%, respectively, during the cation adsorption process. Although the experimental molecular weight is very close to the molecular weight of hydronium, according to the Grotthuss mechanism (conductivity via proton hopping), H_3O^+ adsorption is not likely to be the dominant process in acidic electrolyte vs proton adsorption [36]. Based on the discussion above, it is confirmed that during charge/discharge process in multi-ion aqueous solution at low pH, both cations (H^+ and K^+) and anions (HSO_4^- and SO_4^{2-}) contribute to the adsorption/desorption process. Since the EMI^+ molecular ionic mobility is the slowest, in part due to its

larger diameter and its higher form factor, EMI^+ cations did not seem to significantly contribute to the adsorption process. Another observation is that the ion mixing zone enlarged with the presence of bulky EMI^+ cation, especially at the negative charge region (red and blue line in Fig. 2d). One possibility is that the bulky cation slow down the access of water or hydronium to the electrode surface during charging [25]. This study shows that EQCM is an effective gravimetric probe to study the composition changes of ionic fluxes and distinguish the main charge carriers during adsorption/desorption with multi-ion aqueous electrolytes in porous materials.

4. Conclusions

In this study, cyclic voltammetry with in situ EQCM measurement has been used to study the ion dynamic in porous carbon electrodes from different aqueous electrolytes. In binary aqueous electrolytes 0.1 M K_2SO_4 and 0.1 M $\text{EMI}^+\text{-HSO}_4^-$, protons were found to be the main charge carrier during negative polarization in $\text{EMI}^+\text{-HSO}_4^-$ electrolyte. In mixed 0.1 M K_2SO_4 and $\text{EMI}^+\text{-HSO}_4^-$ electrolyte, the main charge carriers have been identified to be protons, K^+ , HSO_4^- and SO_4^{2-} during cycling. Moreover, these results show that the change of electrolyte pH changes the main charge carrier during cycling.

Overall, the profile of ionic fluxes was revealed by EQCM in simple and sophisticated electrolyte environment. This approach demonstrates that EQCM served as an advanced analytical method extends our understanding for ion adsorption/desorption in porous carbon material, which is of high importance for designing porous carbon electrodes for supercapacitor applications.

References

- J.A. Turner, A realizable renewable energy future, *Science* 285 (1999) 687–689 (80-), <https://doi.org/10.1126/science.285.5428.687>.
- B.E. Conway, *Electrochemical capacitors: scientific fundamentals and technological applications*, Kluwer Acad. (1999) 698, <http://dx.doi.org/10.1007/978-1-4757-3058-6>.
- R. Kötz, M. Carlen, Principles and applications of electrochemical capacitors, *Electrochim. Acta* 45 (2000) 2483–2498, [http://dx.doi.org/10.1016/S0013-4686\(00\)00354-6](http://dx.doi.org/10.1016/S0013-4686(00)00354-6).
- P. Simon, Y. Gogotsi, Materials for electrochemical capacitors, *Nat. Mater.* 7 (2008) 845–854, <http://dx.doi.org/10.1038/nmat2297>.
- A.G. Pandolfo, A.F. Hollenkamp, Carbon properties and their role in supercapacitors, *J. Power Sources* 157 (2006) 11–27, <http://dx.doi.org/10.1016/j.jpowsour.2006.02.065>.
- Y. Gogotsi, *Carbon Nanomaterial*, (2006).
- P. Simon, Y. Gogotsi, Carbon Å electrolyte systems, *Acc. Chem. Res.* 46 (2013) 1094, <http://dx.doi.org/10.1021/ar200306b>.
- Y. Zhu, S. Murali, M.D. Stoller, K.J. Ganesh, W. Cai, P.J. Ferreira, A. Pirkle, R.M. Wallace, K.A. Cychoz, M. Thommes, D. Su, E.A. Stach, R.S. Ruoff, Supporting material: carbon-based supercapacitors produced by activation of graphene, *Science* 332 (2011) 1537–1541 (80-), <https://doi.org/10.1126/science.1200770>.
- C.R. Pérez, S.H. Yeon, J. Ségalini, V. Presser, P.L. Taberna, P. Simon, Y. Gogotsi, Structure and electrochemical performance of carbide-derived carbon nanopowders, *Adv. Funct. Mater.* 23 (2013) 1081–1089, <http://dx.doi.org/10.1002/adfm.201200695>.
- Y. Gogotsi, A. Nikitin, H. Ye, W. Zhou, J.E. Fischer, B. Yi, H.C. Foley, M.W. Barsoum, Nanoporous carbide-derived carbon with tunable pore size, *Nat. Mater.* 2 (2003) 591–594, <http://dx.doi.org/10.1038/nmat957>.
- R. Dash, J. Chmiola, G. Yushin, Y. Gogotsi, G. Laudisio, J. Singer, J. Fischer, S. Kucheyev, Titanium carbide derived nanoporous carbon for energy-related applications, *Carbon N. Y.* 44 (2006) 2489–2497, <http://dx.doi.org/10.1016/j.carbon.2006.04.035>.
- M. Heon, S. Lofland, J. Applegate, R. Nolte, E. Cortes, J.D. Hettinger, P.-L. Taberna, P. Simon, P. Huang, M. Brunet, Y. Gogotsi, Continuous carbide-derived carbon films with high volumetric capacitance, *Energy Environ. Sci.* 4 (2011) 135–138, <http://dx.doi.org/10.1039/C0EE00404A>.
- P. Huang, M. Heon, D. Pech, M. Brunet, P.L. Taberna, Y. Gogotsi, S. Lofland, J.D. Hettinger, P. Simon, Micro-supercapacitors from carbide derived carbon (CDC) films on silicon chips, *J. Power Sources* 225 (2013) 240–244, <http://dx.doi.org/10.1016/j.jpowsour.2012.10.020>.
- M. Arulepp, J. Leis, M. Lätt, F. Miller, K. Rumma, E. Lust, A.F. Burke, The advanced carbide-derived carbon based supercapacitor, *J. Power Sources* (2006), <http://dx.doi.org/10.1016/j.jpowsour.2006.08.014>.
- J. Chmiola, G. Yushin, Y. Gogotsi, C. Portet, P. Simon, P.L. Taberna, Anomalous increase in carbon capacitance at pore sizes less than 1 nanometer, *Science* 313 (2006) 1760–1763 (80-), <https://doi.org/10.1126/science.1132195>.
- M. Arulepp, L. Permann, J. Leis, A. Perkon, K. Rumma, A. Jänes, E. Lust, Influence of the solvent properties on the characteristics of a double layer capacitor, *J. Power Sources* 133 (2004) 320–328, <http://dx.doi.org/10.1016/j.jpowsour.2004.03.026>.
- M.D. Levi, N. Levy, S. Sigalov, G. Salitra, D. Aurbach, J. Maier, Electrochemical quartz crystal microbalance (EQCM) studies of ions and solvents insertion into highly porous activated carbons, *J. Am. Chem. Soc.* 132 (2010) 13220–13222, <http://dx.doi.org/10.1021/ja104391g>.
- J. Chmiola, C. Largeot, P.L. Taberna, P. Simon, Y. Gogotsi, Desolvation of ions in subnanometer pores and its effect on capacitance and double-layer theory, *Angew. Chem. Int. Ed. Eng.* 47 (2008) 3392–3395, <http://dx.doi.org/10.1002/anie.200704894>.
- D. Aurbach, M.D. Levi, G. Salitra, N. Levy, E. Pollak, J. Muthu, Cation trapping in highly porous carbon electrodes for EDLC cells, *J. Electrochem. Soc.* 155 (2008) A745, <http://dx.doi.org/10.1149/1.2957911>.
- W.-Y. Tsai, P.-L. Taberna, P. Simon, Electrochemical quartz crystal microbalance (EQCM) study of ion dynamics in nanoporous carbons, *J. Am. Chem. Soc.* 136 (2014) 8722–8728, <http://dx.doi.org/10.1021/ja503449w>.
- R. Lin, P.L. Taberna, J. Chmiola, D. Guay, Y. Gogotsi, P. Simon, Microelectrode study of pore size, ion size, and solvent effects on the charge/discharge behavior of microporous carbons for electrical double-layer capacitors, *J. Electrochem. Soc.* 156 (2009) A7–A12, <http://dx.doi.org/10.1149/1.3002376>.
- R.C. Weast, *CRC Handbook of Chemistry and Physics*, (1989), <http://dx.doi.org/10.5860/CHOICE.29-0016>.
- J. Eskusson, A. Jaenes, A. Kikas, L. Matisen, E. Lust, Physical and electrochemical characteristics of supercapacitors based on carbide derived carbon electrodes in aqueous electrolytes, *J. Power Sources* 196 (2011) 4109–4116, <http://dx.doi.org/10.1016/j.jpowsour.2010.10.100>.
- S. Sigalov, M.D. Levi, G. Salitra, D. Aurbach, J. Maier, EQCM as a unique tool for determination of ionic fluxes in microporous carbons as a function of surface charge distribution, *Electrochem. Commun.* 12 (2010) 1718–1721, <http://dx.doi.org/10.1016/j.elecom.2010.10.005>.
- M.D. Levi, S. Sigalov, G. Salitra, D. Aurbach, J. Maier, The effect of specific adsorption of cations and their size on the charge-compensation mechanism in carbon micropores: the role of anion desorption, *ChemPhysChem* 12 (2011) 854–862, <http://dx.doi.org/10.1002/cphc.201000653>.
- R. Futamura, T. Iiyama, Y. Takasaki, Y. Gogotsi, M.J. Biggs, M. Salanne, J. Ségalini, P. Simon, K. Kaneko, Partial breaking of the Coulombic ordering of ionic liquids confined in carbon nanopores, *Nat. Mater.* 16 (2017) 1225–1232, <http://dx.doi.org/10.1038/nmat4974>.
- M.D. Levi, L. Daikhin, D. Aurbach, V. Presser, Quartz crystal microbalance with dissipation monitoring (EQCM-D) for in-situ studies of electrodes for supercapacitors and batteries: a mini-review, *Electrochem. Commun.* 67 (2016) 16–21, <http://dx.doi.org/10.1016/j.elecom.2016.03.006>.
- F. Escobar-Teran, A. Arnau, J.V. García, Y. Jiménez, H. Perrot, O. Sel, Gravimetric and dynamic deconvolution of global EQCM response of carbon nanotube based electrodes by Ac-electrogravimetry, *Electrochem. Commun.* 70 (2016) 73–77, <http://dx.doi.org/10.1016/j.elecom.2016.07.005>.
- B. Dyatkin, O. Gogotsi, B. Malinovsky, Y. Zozulya, P. Simon, Y. Gogotsi, High capacitance of coarse-grained carbide derived carbon electrodes, *J. Power Sources* 306 (2016) 32–41, <http://dx.doi.org/10.1016/j.jpowsour.2015.11.099>.
- J.M. Griffin, A.C. Forse, W.-Y. Tsai, P.-L. Taberna, P. Simon, C.P. Grey, In situ NMR and electrochemical quartz crystal microbalance techniques reveal the structure of the electrical double layer in supercapacitors, *Nat. Mater.* 14 (2015) 812–819, <http://dx.doi.org/10.1038/nmat4318>.
- R. Hanzlik, *Inorganic Aspects of Biological and Organic Chemistry*, Academic Press, New York, 1976.
- A.K. Soper, K. Weckström, Ion solvation and water structure in potassium halide aqueous solutions, *Biophys. Chem.* 124 (2006) 180–191, <http://dx.doi.org/10.1016/j.bpc.2006.04.009>.
- G. Balasubramanian, S. Murad, R. Kappiyoor, I.K. Puri, Structure of aqueous MgSO_4 solution: dilute to concentrated, *Chem. Phys. Lett.* 508 (2011) 38–42, <http://dx.doi.org/10.1016/j.cplett.2011.04.010>.
- A.G. Volkov, S. Paula, D.W. Deamer, Two mechanisms of permeation of small neutral molecules and hydrated ions across phospholipid bilayers, *Bioelectrochemistry Bioener.* 1997, pp. 153–160, [http://dx.doi.org/10.1016/S0302-4598\(96\)05097-0](http://dx.doi.org/10.1016/S0302-4598(96)05097-0).
- E.R. Nightingale, Phenomenological theory of ion solvation. Effective radii of hydrated ions, *J. Phys. Chem.* 63 (1959) 1381–1387, <http://dx.doi.org/10.1021/j150579a011>.
- D. Marx, Proton transfer 200 years after Von Grothuss: insights from ab initio simulations, *ChemPhysChem* 7 (2006) 1849–1870, <http://dx.doi.org/10.1002/cphc.200600128>.
- I.A. Riddell, T.K. Ronson, J.K. Clegg, C.S. Wood, R.A. Bilbeisi, J.R. Nitschke, Cation and anion-exchanges induce multiple distinct rearrangements within metallo-supramolecular architectures, *J. Am. Chem. Soc.* 136 (2014) 9491–9498, <http://dx.doi.org/10.1021/ja504748g>.